β-glucan reprograms alveolar macrophages via neutrophil/IFNγ axis to promote lung injury

Renaud Prével[a], Erwan Pernet[a], Kim A Tran[a], Abderrahmane Sadek[b,c], Mina Sadeghi[a], Elizabeth Lapshina[a], Leonardo Jurado[a], Arnold S. Kristof[a], Mohieddine Moumni[b], Jérémie Poschmann[c], Maziar Divangahi[a,d,e,f,*]

[a] Department of Medicine, Meakins-Christie Laboratories, Research Institute McGill University Health Centre, McGill University, Montreal, Quebec, Canada

[b]Biotechnology and Bioresources Valorization Laboratory, Biology Department, Faculty of Sciences, Moulay Ismail University of Meknès, Meknès, Morocco

[c]INSERM, Nantes Université, Center for Research in Transplantation and Translational Immunology (CR2TI), UMR 1064, ITUN, Nantes, France

[d]Department of Microbiology and Immunology, Meakins-Christie Laboratories, Research Institute McGill University Health Centre, McGill University, Montreal, Quebec, Canada

[e]Department of Pathology, Research Institute McGill University Health Centre, McGill University, Montreal, Quebec, Canada

[f]McGill International TB Centre, Montreal, Quebec, Canada

*Corresponding author: maziar.divangahi@mcgill.ca

Keywords: acute lung injury; trained immunity; alveolar macrophages; neutrophils

ABSTRACT

Alveolar macrophages (AMs) reside in the lower airways and play a crucial role in lung health and response to sterile inflammation and infections. AMs possess remarkable adaptability to different environmental challenges that can persist through their memory capacity (trained immunity). β-glucan has been characterized as a potent inducer of trained immunity by reprogramming hematopoietic stem cells (HSCs) in the bone marrow generating trained innate cells with enhanced responsiveness. In the present study, we show that systemic administration of β-glucan reprograms alveolar macrophages (AMs) in the lung via neutrophils and IFNγ signalling, in a Dectin1-independent manner. We furthermore demonstrate that AM reprogramming at both the transcriptional and metabolic levels exacerbate lung injury following bacterial (LPS) or viral (polyI:C) challenges. These findings identify an additional facet of β-glucan in trained immunity involving AM reprogramming and shed light on the potential detrimental effects of trained immunity.

INTRODUCTION

Sepsis, a life-threatening condition resulting from the host's overwhelming response to infection, continues to pose significant challenges in clinical management and remains a leading cause of mortality worldwide[1]. Among the various triggers of sepsis, lipopolysaccharide (LPS), a component of the outer membrane of Gram-negative bacteria, is a potent inducer of systemic inflammation[2]. Excessive inflammation associated with sepsis causes tissue damage, organ dysfunction, and ultimately, mortality[3, 4]. Thus, the magnitude of inflammatory responses must be regulated to resolve infections while preventing collateral tissue damage. Understanding the mechanisms underlying the regulation of inflammation in sepsis is essential for the development of effective therapeutic interventions. Key players in this regulatory network include various immune cells, cytokines, and signalling pathways, which collectively modulate the intensity and duration of inflammatory responses. Dysregulation of these mechanisms can lead to either persistent inflammation or immunosuppression, both of which contribute to the pathogenesis of sepsis [5, 6, 7].

The constant exposure of the lungs to a non-sterile environment leads to the development of a unique immunity by eliminating inhaled foreign particles while minimizing inflammatory-mediated tissue damage. Resident alveolar macrophages (AMs) serve a crucial regulatory function to maintain the delicate balance between inflammation and protecting lung tissue from damage [8]. AMs originate from fetal liver monocytes and act as vigilant sentinels protecting the airways against invading pathogens and pollutants[9 10]. Thus, AMs play a pivotal role in orchestrating both the initiation and resolution of immune responses within the lung microenvironment.

Adaptations in innate immune cells are diverse with substantial plasticity to various insults that can be maintained resulting in enhanced (trained immunity) or reduced (tolerance) inflammatory responses to a second stimuli [11, 12, 13]. Trained immunity is mediated *via* long-term metabolic reprogramming and epigenetic modifications, which can be induced by various stimuli such as the attenuated mycobacteria Bacille Calmette-Guérin (BCG) or β-glucan (a polysaccharidic component of fungi cell wall)[11, 14]. BCG and β-glucan are able to train monocytes and neutrophils with beneficial impact in cancer or infections *via* the reprogramming of haematopoietic stem cells (HSC) within the bone marrow[15, 16 17, 18]. However, there are substantial knowledge gaps in our understanding of trained immunity within tissue-resident macrophages (TRMs) and its regulatory role in maintaining tissue homeostasis under stress conditions. For instance, while the initial LPS-stimulation of macrophages induces a strong inflammatory responses via TLR-4, restimulation with LPS generates tolerance in these macrophages[19]. Thus, the epigenetic reprogramming of innate immune cells and their subsequent responses depends on two signals: the initial training agent and the nature of the second stimuli at an inflammatory site. Here we showed that systemic administration of β-glucan can reprogram AMs in the lungs via neutrophil/type II IFN axis but independent of Dectin-1 signalling. The unique transcriptomic and metabolic profile of AMs render them hyperresponsive to both bacterial or viral stimulation causing dysregulated inflammatory responses with pulmonary damage. The differences in the systemic basal levels of β-glucan in sepsis patients as well as the pulmonary levels of IFNγ can be major factors in determining the hyperresponsiveness in sepsis patients and can be potentially targeted for therapy.

RESULTS

β-glucan-mediated trained immunity aggravates LPS-induced ALI.

To investigate whether systemic administration of β-glucan induces trained immunity within the lung, we sought to assess its impact on Acute Lung Injury (ALI) triggered by LPS treatment. We initially evaluated the consequences of β-glucan-mediated training on ALI by administering LPS seven days after training (Figure 1A). ALI assessment conducted 24 hours post-LPS instillation did not reveal any discernible distinctions attributable to the initial i.p. β-glucan injection. However, ALI was notably exacerbated in mice that had undergone β-glucan training upon subsequent LPS stimulation as demonstrated non-invasively by lung microCT scanners with regards to the increased proportion of poorly- or non-aerated lung segment and to a significant increase in Hounsfield units (Figure 1B). Hounsfield units reflect a coefficient of tissue attenuation and, by extrapolation, tissue composition. Consistent findings were corroborated through two complementary invasive evaluations of ALI. Specifically, the heightened alveolar-capillary permeability following LPS instillation in β-glucan-trained mice was substantiated by elevated lung Evans blue dye concentrations (Figure 1C). Histological examination further unveiled a spectrum of notable alterations following LPS instillation, including cellular infiltration, thickened alveolar walls, and the formation of hyaline membranes, observed in β-glucan-trained mice and not PBS controls (Figure 1D). The observed cell infiltration 24 hours after LPS instillation was due to a significant recruitment of neutrophils, as assessed in the bronchoalveolar lavage (BAL; $CD11b^{+}Ly6G^{+}$). Strikingly, the frequency and total numbers of neutrophils was doubled in the β-glucan-treated mice, after LPS administration (Figure 1E). Concomitant with the increased neutrophil recruitment, CXCL1[20] was significantly increased in β-glucan-treated mice when compared to control mice after LPS treatment (Figure 1F). Amplified ALI in β-glucan-trained mice was also associated with increased proinflammatory cytokines (IL-6 and TNFα) (Figure 1G-H). As AMs are major

producers of CXCL1, IL6 and TNFα, we next assessed whether β-glucan increased the proportion or number of AMs and found no significant differences between naïve and β-glucan trained mice (Figure 1I). This suggests that that enhanced cytokine production was not due to an increased number of AMs, but rather intrinsic functional changes.

Next, we examined whether the effects of β-glucan-induced immune training persisted in ALI severity. To do so, we administered β-glucan or PBS (control) in mice and after 28 days challenged them with LPS (Supplementary Figure 1A). Similar to the 7-day timeframe of β-glucan training, there was increased endothelial permeability of the lungs (Supplementary Figure 1B), and increased immunopathology (Supplementary Figure 1C) in 28-days β-glucan mice challenged with LPS. This increased ALI in β-glucan treated mice after 28 days was associated with a higher concentration of CXCL1, IL6 and TNFα (Supplementary Figure 1D) and increased neutrophil infiltration in BAL (Supplementary Figure 1E) following LPS instillation. The frequency and number of AMs were not changed between groups (Supplementary Figure 1F). Increased production of cytokines was also observed upon *ex* vivo stimulation of AMs isolated from treated mice 28-day post-β-glucan (Supplementary Figure 1G-H). Thus, the intrinsic functional changes in AMs suggest that the exacerbation of ALI induced by β-glucan triggered a long-term reprogramming of immune cells rather than an additive effect of lingering inflammation from β-glucan injection. To assess whether this response was specific to bacterial LPS or viral agonists can cause similar responses, we next challenged β-glucan trained mice with a TLR-3 agonist (poly(I:C)) (Supplementary Figure 2A). Similar to the LPS-model, β-glucan treated mice had heightened poly(I:C)-induced ALI shown via increased alveolar-capillary permeability, tissue damage, pro-inflammatory cytokine, and neutrophil infiltration (Supplementary Figure 2B-E). In the poly(I:C) model, the number of AMs was also unchanged among groups (Supplementary Figure 2F). Collectively,

these results suggest that systemic β-glucan can maintain a long-term reprogramming in innate immune cells promoting ALI.

β-glucan augmented ALI is mediated via AM

Although there were no differences in the frequency or absolute number of AMs between β-glucan-treated and control mice, the early heightened response with increased CXCL1 production and the recruitment of neutrophils indicate that the AMs are engaged in the exacerbation of ALI induced by β-glucan. To further characterize the role of these cells in ALI, we locally depleted AMs using intranasally administered clodronate liposomes 2 days before performing the LPS instillation, which is at its peak of AM depletion (Figure 2A). Depletion of AMs significantly reduced the production of cytokines TNFα, IL-6, and CXCL1 and the recruitment of neutrophils in BAL, which abolished the β-glucan-induced ALI (Figure 2B-D). To further confirm that tissue-resident AMs are responsible for the increased β-glucan-induced ALI, we used *Csf2rb*$^{-/-}$ mice (Figure 2E), which do not naturally develop alveolar macrophages throughout their lifespan but maintain regular levels of bone marrow derived macrophages (BMDMs) and interstitial macrophages[21]. Similar to the AM depletion, the production of cytokines and neutrophil recruitment in BAL was similar between β-glucan treated and control *Csf2rb*$^{-/-}$ mice after LPS administration. Importantly, there was no difference in ALI, as similar levels of proteins were measured in the BAL of β-glucan treated and control *Csf2rb*$^{-/-}$ after the LPS challenge (Figure 2F-H).

To complement these loss-of-function experiments with a gain-of-function, we adoptively transferred AMs from adult WT control (PBS) or trained (β-glucan) mice to day 2 *Csf2rb*$^{-/-}$ pups (Figure 2I) and after 6 weeks challenged these mice with LPS. Remarkably, mice replenished with AMs from β-glucan-trained mice displayed an increased in production of inflammatory cytokines and the recruitment of neutrophils into the BAL (Figure 2K, L). This

was associated with increased ALI as they had higher protein levels in their BAL compared to mice who received control AMs (Figure 2J). Collectively, our data demonstrate that the exacerbation of LPS-induced ALI in β-glucan-trained mice is mediated through AMs, mainly via functional reprogramming rather than a change in quantity or proportion.

β-glucan reprograms AM

Our findings indicate that β-glucan reprograms AMs causing an increased response to LPS and subsequently enhanced ALI. To test this hypothesis, we investigated the transcriptional state of AMs after seven days training with β-glucan *in vivo*, which were then stimulated with/without LPS *ex vivo* LPS. The rationale for using an *ex vivo* system was to ensure that AMs are uniformly stimulated with LPS (Figure 3A).

Principal component analysis (PCA) of all expressed genes across the four conditions revealed that control and β-glucan trained AMs had distinct transcriptional profiles (Figure 3B). More precisely, the 4 different conditions explained the largest variance as they spread out across the first principal component (PC), while the variation within replicates was associated to the second and third PC. Next, we investigated the effect of β-glucan trained AMs by comparing the differential gene expression between control and β-glucan treated mice (Figure 3C). We found 88 differentially expressed genes (32 up-regulated and 56 down-regulated, with a false discovery rate (FDR) adjusted p value < 0.05 and a log2fold-change cut-off of 1). Despite that only few genes were differentially expressed, gene ontology analysis indicated a strong enrichment of genes involved in innate immune response and defense response to virus (Figure 3D). Interestingly, LPS response genes were downregulated in β-glucan-treated mice suggesting that, in response to β-glucan, the LPS response pathway is attenuated or less activated. Gene set enrichment analysis (GSEA) additionally revealed an increase of genes involved in IFNα but a significant decrease of genes involved in TNFα signalling (Figure 3E).

Next, we explored how *ex vivo* stimulated AMs responded to LPS using the same differential gene expression analysis. LPS altered the expression of 525 genes (FDR >0.05 log2FC >1.5) with the up regulation of 438 genes including numerous pro-inflammatory genes (Figure 3F). As expected, gene ontology analyses revealed that these genes were involved in cellular response to LPS, inhibition of viral genome replication, production of interleukin-1β and cellular response to IL-1 (Figure 3G). Additional analysis of GSEA indicated up-regulation of genes involved in TNFα signalling (Figure 3H), indicating that LPS and β-glucan both induce interferon responses but have opposite effects on the TNF response pathway.

To delineate how β-glucan training of AMs may affect the subsequent response to LPS, we then compared the fold change of gene expression in response to LPS stimulation between β-glucan trained and untrained AMs. Notably, we observed an upregulation of genes associated with the LPS response (depicted in blue) in the β-glucan trained group (Figure 3I). This heightened response included a significant increase in the expression of IL-6, IL-1, TNF, and other genes (Figure 3I, J). This increased response to LPS by β-glucan-trained AMs was confirmed at the protein level as they exhibited increased *ex vivo* production of CXCL1 and TNFα (Figure 3K). Such an increased response to LPS was also obtained in AMs after 28 days β-glucan training (Supplementary Figure 1G). We also observed similar trends in genes associated with the defense response to viruses (Supplementary Figure 2G) which is in line with our findings showing an increased ALI to poly(I:C) (Supplementary Figure 2B-D). Taken together, β-glucan reprograms AMs to respond robustly to LPS stimulation.

As trained immunity is associated with metabolic rewiring, we next assessed if β-glucan-induced training modified the AM's metabolic state. Genes involved in both oxidative phosphorylation and glycolysis were up-regulated during response to LPS in β-glucan-trained AMs compared to untrained AMs but not at the steady state (Figure 3L). The Seahorse assay showed while only mitochondrial respiration was increased in β-glucan-trained AMs at the

steady state, both mitochondrial respiration and glycolysis were increased during the response to LPS in β-glucan-trained AMs, (Figure 3M). Taken together, β-glucan functionally reprograms AMs by rewiring their transcriptomic and metabolic states.

IFNγ signaling and neutrophils are required for AM reprogramming

Dectin-1 is the receptor that recognizes β-glucan and is involved in mediating the biological effects of β-glucan-induced training in most cell types[14]. To assess the role of Dectin-1 in β-glucan increased LPS-induced ALI, we used the same experimental setup using Dectin-1 deficient mice (Supplementary Figure 3A). Surprisingly, the increased neutrophil infiltration and pro-inflammatory cytokine production in BAL were maintained in β-glucan-treated *Dectin-1*$^{-/-}$ mice and there was no change in the AM numbers (Supplementary Figure 3B-D). To determine the effect of Dectin-1 on β-glucan-induced AM function, *Dectin-1*$^{-/-}$ mice were treated with β-glucan and after 7 days AMs were cultured and stimulated *ex vivo* with LPS (Supplementary Figure 3E). Similar to wild-type AMs, the production of pro-inflammatory cytokines CXCL1 and TNFα was increased in β-glucan-trained Dectin1-deficient AMs after LPS stimulation (Supplementary Figure 3F). This indicates that β-glucan-induced AMs reprogramming is Dectin-1-independent and that AMs are trained via a different signalling pathway. Since we observed type I IFN gene expression is increased in AMs after β-glucan treatment (Figure 3E) and type I IFN was previously reported to be involved in AMs training[22], we next assessed the impact of β-glucan on AMs reprogramming in *IfnaR*$^{-/-}$ mice, which lack type I IFN signalling (Supplementary Figure 3G). Similar to Dectin-1 deficient mice, increased production of pro-inflammatory cytokines in response to LPS by β-glucan-treated *IfnaR*$^{-/-}$ AMs was maintained, demonstrating that β-glucan-induced AMs reprogramming is type I IFN-independent (Supplementary Figure 3H).

Considering recent studies suggesting type II IFN can train AMs following BCG [23] or adenoviral infection [24], using *IfngR*$^{-/-}$ mice we next investigated if type II IFN is involved in β-glucan-induced exacerbation of ALI (Figure 4A). In contrast to *Dectin1*$^{-/-}$ *or IfnaR*$^{-/-}$ mice, the increased neutrophils recruitment, inflammatory cytokines production, and ALI were abolished in β-glucan-trained *IfngR*$^{-/-}$ mice (Figure 4B-D). To investigate the role of type II IFN signalling in β-glucan-induced reprogramming of AMs, we performed *ex vivo* LPS stimulation on β-glucan trained *IfngR*$^{-/-}$ AMs (Figure 4E). The increase of inflammatory cytokines in response to LPS by β-glucan-trained AMs was abolished (Figure 4F), suggesting that training of AM by β-glucan is IFNγ-dependent.

Considering the concentration of IFNγ was significantly increased in BAL at day 1 post- β-glucan administration, which was associated with the increased number of neutrophils (Figure 4G-J), we next assess the direct role of IFNγ in training of AMs by β-glucan. We selectively depleted IFNγ prior to β-glucan administration *in vivo* (Figure 4K), and found the production of inflammatory cytokines (CXCL1 and TNFα) was significantly reduced in β-glucan trained AMs. Similarly, the depletion of neutrophils prior to β-glucan treatment in mice resulted in significant reduction in inflammatory cytokines in β-glucan trained AMs (Figure 4L). These findings indicate that β-glucan reprograms AMs via IFNγ- and neutrophils-dependent manner.

DISCUSSION

The evolving field of trained immunity has challenged the boundaries we once drew to discern between the innate and adaptive immune systems. The discovery that the innate immune system can be 'trained' to retain memory-like features has provided novel avenues for prophylactic and therapeutic strategies. The use of an adjuvant like β-glucan has been investigated as an anti-infection agent in acute infections or inflammatory conditions [15, 25] as well as an anti-cancer treatment [26, 27]. While we and others have shown that β-glucan can induce central trained immunity by functionally reprogramming the hematopoietic stem cell compartment in the bone marrow, the present study highlights an additional facet of β-glucan's immunomodulatory effects on residential immune cells. Here we show that a single intraperitoneal (i.p.) injection of β-glucan can induce trained immunity in the lung alveolar macrophages and functionally reprograms AMs at both the transcriptional and metabolic levels. These findings underscore the occurrence of tissue-specific immune training following systemic treatment, demonstrating processes of β-glucan-mediated peripheral trained immunity occurring in parallel with central immunity. We subsequently demonstrate that β-glucan trained AMs can be detrimental after LPS or poly(I:C) administration causing severe ALI. Thus, this study is shedding light on the deleterious effects of trained immunity and its impact on immunopathology, which is incompletely understood.

There are several key features in trained immunity, including shifts in epigenetic and transcriptomic profiles after initial stimulation that returns to steady states. However, this epigenetic and metabolic remodeling result in long-term memory with heightened responses to diverse secondary stimulation [11]. Therefore, two signals are required for the induction of trained immunity: signal 1, which is essential for reprogramming innate immune cells, and signal 2, an environmental cue critical for activating their functional capacity. In this study, we provide evidence supporting this conceptual framework.

β-glucan-trained AMs were able to generate a robust response both *in vitro* and *in vivo* to bacterial (LPS) or viral (poly(I:C)) ligands. The increased response in β-glucan-trained AM was maintained up to 28 days, which is an indication of long-term reprogramming of AMs. The reprogramming of trained AMs was supported by significant alterations in both the transcriptomic and metabolic states. Using adoptive transfer experiments, we then showed that the functional reprogramming of β-glucan trained AMs persisted even in the absence of the initial systemic β-glucan administration. This finding highlights the persistence of the intrinsic training program in AMs.

AMs are originated from yolk sac and fetal liver monocytes, which seeds the lung as soon as we take our first breath of air [9]. Importantly, AMs are the first immune cell to response to any particles or pathogens that reach the lower airways of the lungs, thus alterations in their functional capacity can significantly impact subsequent immune responses. For instance, given AMs are in direct contact with surfactant (produced by alveolar type 2 epithelial cells) and invading pathogens, a defect in GM-CSF or TGFβ signalling leads to accumulation of surfactant (alveolar proteinosis) and increased susceptibility to pulmonary infections[28, 29]. AMs are able to sense and integrate multiple environmental signals - such as pH[29], temperature[30, 31], osmolarity[32], metabolites including fatty acids[33, 34], extracellular membrane components and danger signals [35] – to maintain tissue homeostasis[36]. However, the mechanisms underlying their ability to adapt to environmental stimuli while maintaining lung tissue homeostasis without impairing gas exchange is largely unknown[37]. AMs exhibit a remarkable plasticity, demonstrating a spectrum of functional polarization that ranges from regulatory to pro-inflammatory and anti-inflammatory states. For instance, AM anti-inflammatory polarization in a LPS model of sepsis was TNFα dependent, as AMs exposed to TNFα exhibited diminished phagocytosis, superoxide anion (O2-) and CXCL1 production, with reduced neutrophils recruitment[38]. Consequently, these mice had a reduction in lung clearance of *P. aeruginosa*

infection. Influenza virus was able to induce similar anti-inflammatory function in AMs with decreased CXCL1 production and neutrophils recruitment via type I IFN pathway[39], leading to an increased susceptibility to super bacterial infection. On the other hand, AMs appear to be more resistant to polarization towards a pro-inflammatory state [40]. A recent study demonstrated that exposure of lungs to ambient amount of LPS trains AMs in type I IFN dependent, but type II IFN and T cell independent manner[22]. However, in our model system, systemic administration of β-glucan trains AMs in a type II IFN dependent, but type I IFN independent manner. Similarly, in live infection models, we and others have identified IFNγ signaling a key player in AM training after BCG vaccination[23], influenza infection[41], pneumococcal infection [42] and intranasal infection with an adenoviral vector [8]. Although we have not identified which cells produce IFNγ in the β-glucan model, it has been demonstrated by our group and others that following BCG vaccination, CD4+ T cells are the major source of IFNγ [23], whereas after pulmonary adenovirus infection, CD8+ T cells predominantly produce IFNγ [24]. Influenza infection has also been described to induce IFNγ-dependent AM training with NK cells being the major source [41]. Interestingly, we found that neutrophils were also required for β-glucan-mediated AMs training. It has been shown that β-glucan can reprogram HSCs to promote granulopoiesis and the generation of trained neutrophils [27]. Although we have shown that the recruitment of these trained neutrophils into the lung was required for training AMs, the cellular and molecular mechanisms involved in this dialogue is unknown and requires further investigation. Interestingly, we have recently demonstrated that, in addition to GM-CSF and TGFβ signalling, neutrophils are critical for AMs self-renewal and maintenance during early lung development *via* the production of 12-hydroxyeicosatetraenoic acid (12-HETE)[43]. The absence of 12-HETE leads to a significant reduction in the number AMs in adult lungs, enhanced senescence, and consequently increased susceptibility to IAV or SARS-CoV-2 infection. Thus, there might be a constant bidirectional dialogue between neutrophils and AMs,

with neutrophils providing cues from internal organelles to AMs, and AMs offering signals from the external environment to neutrophils, which then return to their graveyard in the BM.

Although we have not directly tested the contribution of circulating monocytes in the initial reprogramming of AMs via β-glucan, the persistence of trained immunity by adoptively transferred AMs into *Csf2rb*$^{-/-}$ mice suggests that the maintenance of the trained AM state was independent of bone marrow derived monocytes. Additionally, the findings from Theobald *et al* indicate that Dectin-1 is the receptor responsible for recognizing β-glucan which has been shown to activate macrophages and induce trained immunity in several models [44, 45, 46]. Here we found that β-glucan-mediated AM training, when administered systemically, was independent of Dectin-1. There are two potential explanations for this observation. First, it has been shown that β-glucan can also activate signaling via other TLRs, particularly TLR2 or complement receptor 3 (CR3) [47, 48, 49], and second as the β-glucan is a particulate, its internalization by phagocytes can also initiate signaling [50, 51, 52]. Additionally, our understanding of how administration of β-glucan in peritoneal cavity leads to HSCs training in the BM and AMs training in thoracic cavity is extremely limited. Thus, addressing the molecular mechanisms of β-glucan signaling pathways (e.g., Dectin1-dependent and independent) in both immune and non-immune cells, as well as its mode of action (e.g., direct access to an organ versus indirect effects via systemic release of cytokines), is necessary to delineate the deleterious versus protective effects of β-glucan-mediated trained immunity.

β-glucan is present in the cell wall of all fungi but will vary between different species and strains. In fact, the differential 1,3 to 1,6 glycosidic branching and molecular weight significantly impacts the response to the compound with a large variability of scientific findings contingent on the type of β-glucan used in a study[53, 54, 55]. Fungi make up a portion of the human microbiome, termed the mycobiome. Several studies have described a high mycotic diversity

between different populations, and even significant variability within an individual overtime [56, 57, 58]. The variance in gut colonization by fungal species can moreover cause gut dysbiosis which has been associated with poorer outcomes during SARS-CoV-2 infection, sepsis and cancer immunotherapy[59, 60 61, 62, 63]. It is tempting to postulate that the levels of the mycobiome as well as its composition can influence subsequent immune reactions partly due to a distinct β-glucan makeup. In fact, antibodies to various types of β-glucan was detected in adult sera with different levels correlating with a person's occupation [64]. Thus, the quantity and quality of circulating β-glucan in an individual at steady state can remarkably affect the subsequent immune responses to sterile or microbial inflammation. This mechanism(s) provides a basis for host response heterogeneity in sepsis-induced ALI and how basal levels of β-glucan can play a role in excessive inflammation [65]. Understanding these underlying processes may provide important insights for developing novel therapeutic approaches in sepsis.

MATERIALS AND METHODS

Mice

C57BL/6, *Csf2rb*$^{-/-}$, *Dectin1*$^{-/-}$, *IfnaR*$^{-/-}$ and *IfngR*$^{-/-}$ mice were purchased from Jackson Laboratories. All animals were housed and inbred at the animal facility of the Research Institute of McGill University under specific pathogen-free conditions with *ad libitum* access to food and water, a temperature of 21 °C (±1 °C), relative humidity of 40–60% (±5%) and light cycle of 12 h on, 12 h off (daily cycle). *Sex as a biological variable*: Mice were randomly allocated to experimental groups, and experiments were performed using both female and male age- and sex-matched mice. Similar findings were reported for both sexes.

β-glucan training

Mice were administered intraperitoneally with 1mg of β-1,3-glucan purified from *Saccharomyces cerevisiae* (Sigma) diluted in 100µL of PBS seven days or twenty-eight days before lung injury or AMs collection for *ex vivo* stimulation.

Acute lung injury models

Mice were administered with 50µg of *Escherichia coli* O55:B55 LPS (Sigma) or poly(I:C) (Invivogen) in PBS (25 µL per mouse, intranasally) to induce TLR-4 or 3-mediated acute lung injury (ALI), respectively.

Lung microCT scan

The trachea was cannulated with a 22-gauge cannula and an intra-thoracic pressure of 25mmH_2O was generated using a manometer. Images were acquired right after lung inflation using the nanoScan SPECT + CT (Mediso®) allowing a resolution of 20µm. DICOM software

was used to analyse the microCT scans determining the average lung Hounsfield unit (HU) and the proportion of non- or poorly-aerated lung (HU -500; +100).

BAL and lung collection

Broncho-alveolar lavage (BAL) samples collected by cannulating the trachea with a 22-gauge cannula, then washing the lungs with 3× 1 mL of cold, sterile PBS. The total volume of the recovered fluid after lavage was around 0.7 ml. Samples were centrifuged (1,500 r.p.m., 10 min). Lung tissues were perfused with 10 mL of PBS, collected and minced before collagenase type I (3mg, Worthington CLS-1), elastase (3mg, Worthington ESL) and DNase I (0.4mg, Worthington D) digestion for 30min at 37 °C. Lungs were filtered through a 70 µm nylon mesh, and red blood cells were lysed.

Endothelial permeability

LPS or poly(I:C)-challenged mice were intravenously injected with 400 µl of Evan's blue dye (2% in PBS) into the mice. After 1 h, mice were euthanized, and lungs were perfused with 10 ml of PBS. Evan's blue then extracted by overnight incubation in formamide at 56 °C (lungs) and quantified by spectrophotometry analysis using a standard curve of Evan's blue in formamide.

Histopathological analysis

Histopathological analysis was performed as previously described[43]. Lungs were inflated and fixed for 48 h with 10% formalin, and then embedded in paraffin. Sections (5 µm) were cut and stained with haematoxylin and eosin. Slides were scanned at a resolution of ×40 magnification, and pictures were taken using a Leica Aperio slide scanner (Leica).

ELISA

CXCL1, TNF-α, IL-6 and IFNγ levels in BAL were assessed by ELISA (R&D Systems).

Protein in BAL

Samples were centrifuged (1,500 r.p.m., 10 min), and total protein content was assessed using a Pierce BCA Protein assay (ThermoFisher).

Flow cytometry

BAL and total lung cell counts were determined with a haemocytometer, and 1–2 million cells were used for staining. Cells were initially stained with viability dye e506 (Invitrogen, 20 min, 4 °C) and surface stained with anti-CD16/32 (BD Bioscience) in 0.5% BSA/PBS solution to block nonspecific AB interaction with Fc receptors (10 min, 4 °C). Cells were then surface-stained with different combinations of PE-Cy7-conjugated anti-CD11c, BUV786-conjugated anti-Siglec-F, BUV395-conjugated anti-CD11b, APC-Cy7-conjugated anti-Ly6G, BUV737-conjugated anti-CD45.2 antibodies (all from BD Biosciences). For IFNγ intra-cellular staining, cells were fixed and permeabilized using BD CytoFix/CytoPerm (BD Bioscience) before intracellular staining with PE-conjugated anti-IFNγ antibodies (BD Biosciences). Flow cytometry was performed using a BD LSR Fortessa X-20 instrument (BD Biosciences) with FACSDiva software v.8.0.1 (BD Biosciences). Analysis was performed using FlowJo software v.10.7.1 (Tree Star).

Intravascular staining

In vivo discrimination between pulmonary vasculature and parenchyma was performed as previously described[43]. Adult WT mice were given 2 μg of FITC-conjugated anti-CD45.2

intravenously to label all circulating cells. Three minutes later, mice were euthanized and lungs collected, stained *ex vivo* with BUV395-conjugated anti-CD45.2 antibody to determine the parenchymal (cells only labelled with the *ex vivo* antibody) or vascular localization of the cells (cells labelled with both antibodies).

AM depletion

WT mice were treated with control or clodronate liposomes (70 µl, intranasally; Liposoma BV). The LPS-induced ALI was then performed at day 2 after clodronate instillation.

Adoptive transfer models

AMs from WT mice which received i.p. PBS or β-glucan were collected as described above and resuspended at a density of 5×10^4 cells per 5-7 µL of RPMI1640 medium supplemented with 10% (v/v) FBS, 2 mM l-glutamine, 10 mM HEPES and 100 U ml–1 penicillin–streptomycin. AMs were then transferred by the intranasal route into Day 2 *Csf2rb*$^{-/-}$ pups. LPS-induced ALI was performed 6 weeks after AM adoptive transfer. BAL and lung tissue were collected and processed as described above for endothelial permeability, flow cytometry, total BAL cytokine and protein content experiments.

Isolation and culture of alveolar macrophages

AMs were collected by BAL of naive mice using cold, sterile PBS (5 × 1 mL for adult mice). AMs were cultured in the specific media described above. After 1 h of adhesion, AMs were washed with PBS and placed in fresh medium.

Ex vivo *stimulation*

AMs from WT, *Dectin1*$^{-/-}$, *IfnaR*$^{-/-}$ and *IfngR*$^{-/-}$ mice which received i.p. PBS or β-glucan were collected as described above and 5×10^4 cells in specific media were distributed per well. AMs were stimulated with 50 ng/ mL of LPS (Sigma) for 4 hours at 37°C.

Library preparation and RNA-seq

Total RNA was collected from BAL AMs from four WT mice per conditions (i.p PBS, no *ex vivo* stimulation / i.p. β-glucan, no *ex vivo* stimulation / i.p PBS, *ex vivo* LPS stimulation / i.p. β-glucan, *ex vivo* LPS stimulation). After RNA quality controls, sequencing libraries were constructed using the Illumina TruSeq protocol. Libraries were sequenced on an Illumina NovaSeq 6000 (paired-end 100 base pair) to an average depth of 51,189,336 reads per sample.

RNA-seq data analysis

RNA-seq reads were aligned to the Mus musculus genome from Ensembl version 99 using STAR (version 2.7.3a) was used[66]. All regions overlapped between referenced exons and alignments were counted using featureCounts (subread-1.6.4)[67]. Low abundance genes were filtered out leaving 12,894 genes for subsequent analysis.

Differential expression analyses were performed using the DESeq2 package (DESeq2 1.40.2)[68]. Gene ontology analysis was realized with the R package TopGO. For gene set enrichment analysis (GSEA) a ranked list of the differentially expressed genes was used with clusterProfiler v4.8.2[69], and the Molecular Signatures Database MSigDB v7.5.1.

Extracellular flux analysis

Seahorse assay of isolated cells was performed as previously described[43]. Real-time OCRs of AMs were measured in XF medium (non-buffered RPMI containing 2 mM l-glutamine, 25 mM glucose and 1 mM sodium pyruvate) using a Seahorse Xfe 96 Analyzer (Agilent Technologies). For the mitochondrial stress test, mitochondrial inhibitors oligomycin (1.5 μM), fluorocarbonyl cyanide phenylhydrazone (FCCP) (1 μM), antimycin A and rotenone (0.5 μM) were used as per the manufacturer's recommendations. In brief, cells were seeded at a density of 100,000 cells per well and 3 basal measurements were taken. Following this, two consecutive measurements were taken following each injection of oligomycin, FCCP and antimycin A with rotenone. All measurements were normalized to cell number using crystal violet dye extraction assay. Oxygen consumption curves, OCRs and ECARs were generated using Wave Desktop 2.3 (Agilent Technologies).

IFNγ and neutrophils depletion experiments.

Sex- and age-matched adult WT mice received intra-peritoneal 200μg of anti-IFNg (rat IgG1k, Biolegend), anti-Ly6G (rat IgG2a,k, Biolegend) or appropriated control isotypes injection at Day-1, Day 0, Day 2, Day 4 and Day 6 per intraperitoneal injection of β-glucan. AMs collection for *ex vivo* stimulation was performed at Day 7 after intraperitoneal β-glucan injection.

Ethics statement

All experiments involving animals were approved by the McGill University Animal Care Committee (permit number 2010–5860) in accordance with the guidelines set out by the Canadian Council on Animal Care.

Statistical analysis

Data are presented as the median with interquartile range. Statistical analyses were performed using GraphPad Prism v.9.1.2 software (GraphPad). Statistical differences were determined using one-way analysis of variance (ANOVA) followed by Dunn's multiple comparisons test, paired or unpaired two-tailed t-test or two-tailed Mann–Whitney test. Differential gene expression analysis was carried out using DEseq2 package[68].

Data availability

All data supporting the findings of this study are included in the published article and supplementary materials. Bulk RNA-seq data have been deposited to the European Nucleotide Archive and will be made publicly available upon publication. Source data are provided with this paper.

Acknowledgements

The authors acknowledge technical help from staff at the RI-MUHC histopathology platform and RI-MUHC Small Animal Imaging Laboratory. M.D. is funded by Canadian Institute of Health Research (CIHR) Project Grant-168885 and MM1174910, a Fonds de recherche du Québec–Santé (FRQS) Award, holds the Strauss Chair in Respiratory Diseases and is a fellow member of the Royal Society of Canada. E.P. and R.P. are fellows supported by a Postdoctoral Fellowship from the Fonds de Recherche du Québec Santé.

Author contributions

Conceptualization: R.P., E.P. and M.D. Methodology: R.P., E.P., A.S.K., M.S., K.A.T., R.S., E.L., L.J., J.P. and M.D. Investigation: R.P., K.A.S., E.P., J.P. and M.D. Funding acquisition: M.D. Project administration: R.P. and M.D. Supervision: E.P., J.P. and M.D. Writing original

draft: R.P. K.A.T and M.D. Writing, review, and editing: K.A.T, R.P., E.P., K.A.S., J.P. and M.D.

Competing interests

The authors declare no competing interests.

REFERENCES

1. Singer, M. *et al.* The Third International Consensus Definitions for Sepsis and Septic Shock (Sepsis-3). *Jama* **315**, 801-810 (2016).

2. Opal, S.M. Endotoxins and other sepsis triggers. *Contrib Nephrol* **167**, 14-24 (2010).

3. Xu, Y. *et al.* Mechanisms of Sepsis-Induced Acute Lung Injury and Advancements of Natural Small Molecules in Its Treatment. *Pharmaceuticals (Basel)* **17** (2024).

4. Gill, S.E., Rohan, M. & Mehta, S. Role of pulmonary microvascular endothelial cell apoptosis in murine sepsis-induced lung injury in vivo. *Respir Res* **16**, 109 (2015).

5. Sun, B. *et al.* Acute lung injury caused by sepsis: how does it happen? *Front Med (Lausanne)* **10**, 1289194 (2023).

6. Kumar, V. Pulmonary Innate Immune Response Determines the Outcome of Inflammation During Pneumonia and Sepsis-Associated Acute Lung Injury. *Front Immunol* **11**, 1722 (2020).

7. Zhou, X. & Liao, Y. Gut-Lung Crosstalk in Sepsis-Induced Acute Lung Injury. *Front Microbiol* **12**, 779620 (2021).

8. Schneider, C. *et al.* Induction of the nuclear receptor PPAR-γ by the cytokine GM-CSF is critical for the differentiation of fetal monocytes into alveolar macrophages. *Nat Immunol* **15**, 1026-1037 (2014).

9. Guilliams, M. *et al.* Alveolar macrophages develop from fetal monocytes that differentiate into long-lived cells in the first week of life via GM-CSF. *J Exp Med* **210**, 1977-1992 (2013).

10. Hussell, T. & Bell, T.J. Alveolar macrophages: plasticity in a tissue-specific context. *Nat Rev Immunol* **14**, 81-93 (2014).

11. Divangahi, M. *et al.* Trained immunity, tolerance, priming and differentiation: distinct immunological processes. *Nat Immunol* **22**, 2-6 (2021).

587 12. Netea, M.G. *et al.* Defining trained immunity and its role in health and disease. *Nat Rev*
588 *Immunol* **20**, 375-388 (2020).

589
590 13. Netea, M.G. *et al.* Trained immunity: A program of innate immune memory in health and
591 disease. *Science* **352**, aaf1098 (2016).

592
593 14. Camilli, G., Tabouret, G. & Quintin, J. The Complexity of Fungal β-Glucan in Health and Disease:
594 Effects on the Mononuclear Phagocyte System. *Front Immunol* **9**, 673 (2018).

595
596 15. Moorlag, S. *et al.* β-Glucan Induces Protective Trained Immunity against Mycobacterium
597 tuberculosis Infection: A Key Role for IL-1. *Cell Rep* **31**, 107634 (2020).

598
599 16. Kaufmann, E. *et al.* BCG Educates Hematopoietic Stem Cells to Generate Protective Innate
600 Immunity against Tuberculosis. *Cell* **172**, 176-190.e119 (2018).

601
602 17. Roquilly, A. *et al.* Alveolar macrophages are epigenetically altered after inflammation, leading
603 to long-term lung immunoparalysis. *Nat Immunol* **21**, 636-648 (2020).

604
605 18. Broquet, A. *et al.* Sepsis-trained macrophages promote antitumoral tissue-resident T cells. *Nat*
606 *Immunol* **25**, 802-819 (2024).

607
608 19. Foster, S.L., Hargreaves, D.C. & Medzhitov, R. Gene-specific control of inflammation by TLR-
609 induced chromatin modifications. *Nature* **447**, 972-978 (2007).

610
611 20. Wengner, A.M., Pitchford, S.C., Furze, R.C. & Rankin, S.M. The coordinated action of G-CSF
612 and ELR + CXC chemokines in neutrophil mobilization during acute inflammation. *Blood* **111**,
613 42-49 (2008).

614
615 21. Robb, L. *et al.* Hematopoietic and lung abnormalities in mice with a null mutation of the
616 common beta subunit of the receptors for granulocyte-macrophage colony-stimulating factor
617 and interleukins 3 and 5. *Proc Natl Acad Sci U S A* **92**, 9565-9569 (1995).

618
619 22. Zahalka, S. *et al.* Trained immunity of alveolar macrophages requires metabolic rewiring and
620 type 1 interferon signaling. *Mucosal Immunol* **15**, 896-907 (2022).

621
622 23. Tran, K.A. *et al.* BCG immunization induces CX3CR1(hi) effector memory T cells to provide
623 cross-protection via IFN-γ-mediated trained immunity. *Nat Immunol* **25**, 418-431 (2024).

624
625 24. Yao, Y. *et al.* Induction of Autonomous Memory Alveolar Macrophages Requires T Cell Help
626 and Is Critical to Trained Immunity. *Cell* **175**, 1634-1650.e1617 (2018).

627
628 25. Zervopoulou, E. *et al.* Enhanced medullary and extramedullary granulopoiesis sustain the
629 inflammatory response in lupus nephritis. *Lupus Sci Med* **11** (2024).

630
631 26. Vuscan, P. *et al.* Potent induction of trained immunity by Saccharomyces cerevisiae β-glucans.
632 *Front Immunol* **15**, 1323333 (2024).

633
634 27. Kalafati, L. *et al.* Innate Immune Training of Granulopoiesis Promotes Anti-tumor Activity. *Cell*
635 **183**, 771-785.e712 (2020).

636
637 28. Baker, A.D. *et al.* Targeted PPAR{gamma} deficiency in alveolar macrophages disrupts
638 surfactant catabolism. *J Lipid Res* **51**, 1325-1331 (2010).

639
640 29. Huffman, J.A., Hull, W.M., Dranoff, G., Mulligan, R.C. & Whitsett, J.A. Pulmonary epithelial cell
641 expression of GM-CSF corrects the alveolar proteinosis in GM-CSF-deficient mice. *J Clin Invest*
642 **97**, 649-655 (1996).

643
644 30. Kashio, M. *et al.* Redox signal-mediated sensitization of transient receptor potential
645 melastatin 2 (TRPM2) to temperature affects macrophage functions. *Proc Natl Acad Sci U S A*
646 **109**, 6745-6750 (2012).

647
648 31. Link, T.M. *et al.* TRPV2 has a pivotal role in macrophage particle binding and phagocytosis. *Nat*
649 *Immunol* **11**, 232-239 (2010).

650
651 32. Fang, H.Y. *et al.* Hypoxia-inducible factors 1 and 2 are important transcriptional effectors in
652 primary macrophages experiencing hypoxia. *Blood* **114**, 844-859 (2009).

653
654 33. Haldar, K. *et al.* The sputum microbiome is distinct between COPD and health, independent
655 of smoking history. *Respir Res* **21**, 183 (2020).

656
657 34. Okabe, Y. & Medzhitov, R. Tissue-specific signals control reversible program of localization and
658 functional polarization of macrophages. *Cell* **157**, 832-844 (2014).

659
660 35. Sun, L., Wu, J., Du, F., Chen, X. & Chen, Z.J. Cyclic GMP-AMP synthase is a cytosolic DNA sensor
661 that activates the type I interferon pathway. *Science* **339**, 786-791 (2013).

662
663 36. Okabe, Y. & Medzhitov, R. Tissue biology perspective on macrophages. *Nat Immunol* **17**, 9-17
664 (2016).

665
666 37. Lazarov, T., Juarez-Carreño, S., Cox, N. & Geissmann, F. Physiology and diseases of tissue-
667 resident macrophages. *Nature* **618**, 698-707 (2023).

668
669 38. Mason, C.M., Dobard, E., Summer, W.R. & Nelson, S. Intraportal lipopolysaccharide
670 suppresses pulmonary antibacterial defense mechanisms. *J Infect Dis* **176**, 1293-1302 (1997).

671
672 39. Shirey, K.A. *et al.* Influenza "Trains" the Host for Enhanced Susceptibility to Secondary
673 Bacterial Infection. *mBio* **10** (2019).

674
675 40. Tomlinson, G.S. *et al.* Adherent human alveolar macrophages exhibit a transient pro-
676 inflammatory profile that confounds responses to innate immune stimulation. *PLoS One* **7**,
677 e40348 (2012).

678
679 41. Wang, T. *et al.* Influenza-trained mucosal-resident alveolar macrophages confer long-term
680 antitumor immunity in the lungs. *Nat Immunol* **24**, 423-438 (2023).

681
682 42. Arafa, E.I. *et al.* Recruitment and training of alveolar macrophages after pneumococcal
683 pneumonia. *JCI Insight* **7** (2022).

684
685 43. Pernet, E. *et al.* Neonatal imprinting of alveolar macrophages via neutrophil-derived 12-HETE.
686 *Nature* **614**, 530-538 (2023).

687
688 44. Cheng, S.C. *et al.* mTOR- and HIF-1α-mediated aerobic glycolysis as metabolic basis for trained
689 immunity. *Science* **345**, 1250684 (2014).

690
691 45. Arts, R.J. *et al.* Glutaminolysis and Fumarate Accumulation Integrate Immunometabolic and
692 Epigenetic Programs in Trained Immunity. *Cell Metab* **24**, 807-819 (2016).

693
694 46. Quintin, J. *et al.* Candida albicans infection affords protection against reinfection via functional
695 reprogramming of monocytes. *Cell Host Microbe* **12**, 223-232 (2012).

696
697 47. Yadav, M. & Schorey, J.S. The beta-glucan receptor dectin-1 functions together with TLR2 to
698 mediate macrophage activation by mycobacteria. *Blood* **108**, 3168-3175 (2006).

699
700 48. Thornton, B.P., Větvicka, V., Pitman, M., Goldman, R.C. & Ross, G.D. Analysis of the sugar
701 specificity and molecular location of the beta-glucan-binding lectin site of complement
702 receptor type 3 (CD11b/CD18). *J Immunol* **156**, 1235-1246 (1996).

703
704 49. Xia, Y. *et al.* The beta-glucan-binding lectin site of mouse CR3 (CD11b/CD18) and its function
705 in generating a primed state of the receptor that mediates cytotoxic activation in response to
706 iC3b-opsonized target cells. *J Immunol* **162**, 2281-2290 (1999).

707
708 50. McLeish, K.R., Klein, J.B., Coxon, P.Y., Head, K.Z. & Ward, R.A. Bacterial phagocytosis activates
709 extracellular signal-regulated kinase and p38 mitogen-activated protein kinase cascades in
710 human neutrophils. *J Leukoc Biol* **64**, 835-844 (1998).

711
712 51. Yang, H., He, H. & Dong, Y. CARD9 Syk-dependent and Raf-1 Syk-independent signaling
713 pathways in target recognition of Candida albicans by Dectin-1. *Eur J Clin Microbiol Infect Dis*
714 **30**, 303-305 (2011).

715
716 52. Qi, C. *et al.* Differential pathways regulating innate and adaptive antitumor immune responses
717 by particulate and soluble yeast-derived β-glucans. *Blood* **117**, 6825-6836 (2011).

53. Luo, J. *et al.* Purified β-glucans of Different Molecular Weights Enhance Growth Performance of LPS-challenged Piglets via Improved Gut Barrier Function and Microbiota. *Animals (Basel)* **9** (2019).

54. Moerings, B.G.J. *et al.* Continuous Exposure to Non-Soluble β-Glucans Induces Trained Immunity in M-CSF-Differentiated Macrophages. *Front Immunol* **12**, 672796 (2021).

55. Akramiene, D., Kondrotas, A., Didziapetriene, J. & Kevelaitis, E. Effects of beta-glucans on the immune system. *Medicina (Kaunas)* **43**, 597-606 (2007).

56. Sun, Y. *et al.* Population-Level Configurations of Gut Mycobiome Across 6 Ethnicities in Urban and Rural China. *Gastroenterology* **160**, 272-286.e211 (2021).

57. Szóstak, N. *et al.* Host Factors Associated with Gut Mycobiome Structure. *mSystems* **8**, e0098622 (2023).

58. Nash, A.K. *et al.* The gut mycobiome of the Human Microbiome Project healthy cohort. *Microbiome* **5**, 153 (2017).

59. Reinold, J. *et al.* The Fungal Gut Microbiome Exhibits Reduced Diversity and Increased Relative Abundance of Ascomycota in Severe COVID-19 Illness and Distinct Interconnected Communities in SARS-CoV-2 Positive Patients. *Front Cell Infect Microbiol* **12**, 848650 (2022).

60. Chen, Y. *et al.* Association Between Gut Dysbiosis and Sepsis-Induced Myocardial Dysfunction in Patients With Sepsis or Septic Shock. *Front Cell Infect Microbiol* **12**, 857035 (2022).

61. Huang, X. *et al.* Multi-kingdom gut microbiota analyses define bacterial-fungal interplay and microbial markers of pan-cancer immunotherapy across cohorts. *Cell Host Microbe* **31**, 1930-1943.e1934 (2023).

62. Orieux, A. *et al.* The gut microbiota composition is linked to subsequent occurrence of ventilator-associated pneumonia in critically ill patients. *Microbiol Spectr* **11**, e0064123 (2023).

63. Prevel, R. *et al.* Gut bacteriobiota and mycobiota are both associated with Day-28 mortality among critically ill patients. *Crit Care* **26**, 105 (2022).

64. Noss, I. *et al.* IgG to various beta-glucans in a human adult population. *Int Arch Allergy Immunol* **157**, 98-108 (2012).

65. Grasselli, G. *et al.* Pathophysiology of COVID-19-associated acute respiratory distress syndrome: a multicentre prospective observational study. *Lancet Respir Med* **8**, 1201-1208 (2020).

762
763 66. Dobin, A. *et al.* STAR: ultrafast universal RNA-seq aligner. *Bioinformatics* **29**, 15-21 (2013).
764
765 67. Liao, Y., Smyth, G.K. & Shi, W. featureCounts: an efficient general purpose program for
766 assigning sequence reads to genomic features. *Bioinformatics* **30**, 923-930 (2014).
767
768 68. Love, M.I., Huber, W. & Anders, S. Moderated estimation of fold change and dispersion for
769 RNA-seq data with DESeq2. *Genome Biol* **15**, 550 (2014).
770
771 69. Wu, T. *et al.* clusterProfiler 4.0: A universal enrichment tool for interpreting omics data.
772 *Innovation (Camb)* **2**, 100141 (2021).
773
774 70. Rottman, M. *et al.* IFN-gamma mediates the rejection of haematopoietic stem cells in IFN-
775 gammaR1-deficient hosts. *PLoS Med* **5**, e26 (2008).
776
777
778

FIGURE LEGENDS

Figure 1. β-glucan-mediated trained immunity increases LPS-induced ALI. A, Schematic of the β-glucan-induced training seven days before lipopolysaccharide (LPS)-induced acute lung injury (ALI) model. Experiments were performed in sex- and age-matched 10-12 weeks old control (i.p. PBS, white bars) and trained (i. p. β-glucan, green bars) WT mice. **B**, Lung micro-CT scan, percentage of poorly- or non-aerated lung and average lung Hounsfield unit. **C**, Alveolar capillary membrane permeability assessed by lung Evans blue dye concentration. **D**, Lung histology after staining with haematoxylin and eosin. **E**, Quantification of BAL neutrophils frequency (left) and absolute count (right) (gated on single live cells, $CD45.2^+$, $CD11c^-$, $Siglec\text{-}F^-$, $CD11b^+$, $Ly6G^+$). **F**, **G**, **H** BAL chemokine and pro-inflammatory cytokines concentrations (left to right) (CXCL1: chemokine C-X-C motif ligand 1, IL-6: interleukin-6 and TNF-α: tumor necrosis factor α**). I,** Quantification of BAL alveolar macrophages frequency (left) and absolute count (right) (gated on single live cells, $CD45.2^+$, $CD11c^+$, $Siglec\text{-}F^+$). Data were analysed using one-way ANOVA followed by Dunn's multiple comparisons test. * $p<0.05$, *** $p<0.001$.

Figure 2. Systemic administration of β-glucan enhances ALI via AMs. **A**, Schematic of the clodronate-mediated alveolar macrophages (AM) depletion experiments, performed in sex- and age-matched 10-12 weeks old control (i.p. PBS, white bars) and trained (i. p. β-glucan, green bars) WT mice. **B**, Alveolar capillary membrane permeability assessed by lung Evans blue dye concentration. **C**, Quantification of BAL neutrophils frequency (left) and absolute count (right) (gated on single live cells, $CD45.2^+$, $CD11c^-$, $Siglec\text{-}F^-$, $CD11b^+$, $Ly6G^+$). **D**, BAL chemokine C-X-C motif ligand 1 (CXCL1) and pro-inflammatory cytokines (IL-6: interleukin-6 and TNF-α: tumor necrosis factor α) concentrations. **E**, Schematic of the β-glucan-induced training and

lipopolysaccharide (LPS)-induced acute lung injury (ALI) model in sex- and age-matched 6 weeks old control (i.p. PBS, white bars) and trained (i. p. β-glucan, green bars) *Csf2rb*$^{-/-}$ mice. **F**, BAL total protein concentration. **G**, Quantification of BAL neutrophils frequency (left) and absolute count (right) (gated on single live cells, CD45.2^{+}, CD11c^{-}, Siglec-F^{-}, CD11b^{+}, Ly6G^{+}). **H**, BAL CXCL1, IL-6 and TNF-α concentrations. **I**, Schematic of the adoptive transfer of control (i.p. PBS, white bars) or β-glucan-trained (i. p. β-glucan, green bars) AMs collected from adult WT mice to 2 days old *Csf2rb*$^{-/-}$ mice. Lipopolysaccharide (LPS)-induced acute lung injury (ALI) was performed 6 weeks after adoptive transfer. **J**, BAL total protein concentration. **K**, Quantification of BAL neutrophils frequency (left) and absolute count (right) (gated on single live cells, CD45.2^{+}, CD11c, Siglec-F^{-}, CD11b^{+}, Ly6G^{+}). **L**, BAL CXCL1, IL-6 and TNF-α concentrations. Data were analysed using one-way ANOVA followed by Dunn's multiple comparisons test. * $p<0.05$, ** $p<0.01$, *** $p<0.001$.

Figure 3. β-glucan reprograms AMs. A, Schematic of control (i.p. PBS) or β-glucan-trained (i. p. β-glucan) AMs collected from adult WT mice *ex vivo* stimulation with LPS (LPS-: unstimulated, LPS+: stimulated in RNAseq analysis). **B**, Discovery plot. **C**, AM differential expression of genes in response to β-glucan training. **D**, Gene ontology in response to β-glucan training. **E**, GSEA in response to β-glucan training. **F**, AM differential expression of genes in response to LPS stimulation. **G**, Gene ontology in response to LPS stimulation. **H**, GSEA in response to LPS stimulation. **I**, AM gene expression in response to LPS in β-glucan-trained AMs. **J**, Examples of genes expression in response to LPS in control *vs* β-glucan-trained AMs. **K**, Chemokine C-X-C motif ligand 1 (CXCL1) and tumor necrosis factor α (TNF-α) concentrations after *ex vivo* LPS stimulation. **L**, GSEA of oxidative phosphorylation (left) and glycolysis (right) pathways according to β-glucan-training in unstimulated (LPS-) and LPS stimulated (LPS+) AMs. **M**, Evaluation of AM metabolism: basal respiration (upper left), ATP

production (upper right), extracellular acidification rate (ECAR, lower left), oxygen consumption rate (OCR, lower right). Data were analysed using one-way ANOVA followed by Dunn's multiple comparisons test. ** $p<0.01$, *** $p<0.001$.

Figure 4. IFNγ and neutrophils are required in β-glucan-mediated AM reprogramming. **A**, Schematic of the β-glucan-induced training and lipopolysaccharide (LPS)-induced acute lung injury (ALI) model. Experiments were performed in sex- and age-matched 10-12 weeks old control (i.p. PBS, white bars) and trained (i. p. β-glucan, green bars) *IfngR*$^{-/-}$ mice. **B**, Alveolar capillary membrane permeability assessed by lung Evans blue dye concentration. **C**, Quantification of BAL neutrophils proportion (left) and absolute count (right) (gated on single live cells, CD45.2^{+}, CD11c^{-}, Siglec-F^{-}, CD11b^{+}, Ly6G^{+}). **D**, BAL chemokine C-X-C motif ligand 1 (CXCL1) concentration (left) and pro-inflammatory cytokines (IL-6: interleukin-6 – middle- and TNF-α: tumor necrosis factor α –right) concentrations. **E**, Schematic of control (i.p. PBS, white bars) or β-glucan-trained (i. p. β-glucan, green bars) AMs collected from adult *IfngR*$^{-/-}$ mice *ex vivo* stimulation with LPS. **F**, Chemokine C-X-C motif ligand 1 (CXCL1) and tumor necrosis factor α (TNF-α) concentrations after *ex vivo* LPS stimulation. **G**, Schematic of the analysis of the effect of i.p. β-glucan injection on interferon-γ (IFNγ) production and neutrophils expansion before (white bars) and Day 1, Day 3, Day 5 and Day 7 post-injection (green bars). **H**, BAL IFNγ concentrations. **I**, Quantification of BAL neutrophils proportion (left) and absolute count (right) (gated on single live cells, CD45.2^{+}, CD11c^{-}, Siglec-F^{-}, CD11b^{+}, Ly6G^{+}). **J**, Quantification of lung neutrophils proportion (left) and absolute count (right). **K**, Schematic of control (i.p. PBS, white bars) or β-glucan-trained (i. p. β-glucan, green bars) AMs *ex vivo* stimulation with 50ng/mL LPS. AMs were collected from control (i.p. injection of isotypes), neutrophils depleted (i.p. injection of anti-Ly6G antibodies) or IFNγ antibody-depleted (i.p. injection of anti-IFNγ antibodies) adult WT mice. **L**, CXCL1 and TNF-

α concentrations after *ex vivo* LPS stimulation. Data were analysed using one-way ANOVA followed by Dunn's multiple comparisons test. * $p<0.05$, *** $p<0.001$.

Supplementary Figure 1. Long-term effects of β-glucan-mediated trained immunity on LPS-induced ALI. A, Schematic of the β-glucan-induced training twenty-eight days before lipopolysaccharide (LPS)-induced acute lung injury (ALI) model. Experiments were performed in sex- and age-matched 10-12 weeks old control (i.p. PBS, white bars) and trained (i. p. β-glucan, green bars) WT mice. **B**, Alveolar capillary membrane permeability assessed by lung Evans blue dye concentration. **C**, Lung histology after staining with haematoxylin and eosin. **D**, BAL chemokine C-X-C motif ligand 1 (CXCL1) concentration (left) and pro-inflammatory cytokines (IL-6: interleukin-6 (middle) and TNF-α: tumor necrosis factor α (right)). **E**, Quantification of BAL neutrophils frequency (left) and absolute count (right) (gated on single live cells, CD45.2$^+$, CD11c$^-$, Siglec-F$^-$, CD11b$^+$, Ly6G$^+$). **F,** quantification of BAL alveolar macrophages frequency (left) and absolute count (right) (gated on single live cells, CD45.2$^+$, CD11c$^+$, Siglec-F$^+$). **G**, Schematic of control (i.p. PBS, white bars) or 28 days β-glucan-trained (i. p. β-glucan, green bars) AMs collected from adult WT mice *ex vivo* stimulation with LPS. **H**, Chemokine C-X-C motif ligand 1 (CXCL1) and tumor necrosis factor α (TNF-α) concentrations after *ex vivo* LPS stimulation. Data were analysed using one-way ANOVA followed by Dunn's multiple comparisons test. * $p<0.05$, ** $p<0.01$, *** $p<0.001$.

Supplementary Figure 2. β-glucan-mediated trained immunity increases poly(I:C)-induced ALI. A, Schematic of the β-glucan-induced training seven days before poly(I:C)-induced acute lung injury (ALI) model. Experiments were performed in sex- and age-matched 10-12 weeks old control (i.p. PBS, white bars) and trained (i. p. β-glucan, green bars) WT mice. **B**, Alveolar capillary membrane permeability assessed by lung Evans blue dye concentration.

C, Lung histology after staining with haematoxylin and eosin. **D**, BAL chemokine C-X-C motif ligand 1 (CXCL1) concentration (left) and pro-inflammatory cytokines (IL-6: interleukin-6 (middle) and TNF-α: tumor necrosis factor α (right). **E**, Quantification of BAL neutrophils frequency (left) and absolute count (right) (gated on single live cells, CD45.2^{+}, CD11c^{-}, Siglec-F^{-}, CD11b^{+}, Ly6G^{+}). **F,** Quantification of BAL alveolar macrophages frequency (left) and absolute count (right) (gated on single live cells, CD45.2^{+}, CD11c^{+}, Siglec-F^{+}). **G**, Schematic of control (i.p. PBS, white bars) β-glucan-trained (i. p. β-glucan, green bars) AMs collected from adult WT mice *ex vivo* stimulation with LPS. Differential expression of viral defense genes in response to LPS in β-glucan-trained AMs. Data were analysed using one-way ANOVA followed by Dunn's multiple comparisons test. * $p<0.05$, ** $p<0.01$, *** $p<0.001$.

Supplementary Figure 3. β-glucan-mediated AM reprogramming is independent of Dectin-1 and type I interferon signaling. A, Schematic of the β-glucan-induced training seven days before lipopolysaccharide (LPS)-induced acute lung injury (ALI) model. Experiments were performed in sex- and age-matched 10-12 weeks old control (i.p. PBS, white bars) and trained (i. p. β-glucan, green bars) *Dectin1*$^{-/-}$ mice. **B**, BAL chemokine C-X-C motif ligand 1 (CXCL1) concentration (left) and pro-inflammatory cytokines (IL-6: interleukin-6 (middle) and TNF-α: tumor necrosis factor α (right)). **C**, Quantification of BAL neutrophils frequency (left) and absolute count (right) (gated on single live cells, CD45.2^{+}, CD11c^{-}, Siglec-F^{-}, CD11b^{+}, Ly6G^{+}). **D,** Quantification of BAL alveolar macrophages frequency (left) and absolute count (right) (gated on single live cells, CD45.2^{+}, CD11c^{+}, Siglec-F^{+}). **E**, Schematic of control (i.p. PBS, white bars) β-glucan-trained (i. p. β-glucan, green bars) AMs collected from adult *Dectin1*$^{-/-}$ mice *ex vivo* stimulation with LPS. **F**, Chemokine C-X-C motif ligand 1 (CXCL1) and tumor necrosis factor α (TNF-α) concentrations after *ex vivo* LPS stimulation. **G**, Schematic of control (i.p. PBS, white bars) β-glucan-trained (i. p. β-glucan, green bars)

AMs collected from adult *IfnaR*$^{-/-}$ mice *ex vivo* stimulation with LPS. **H**, Chemokine C-X-C motif ligand 1 (CXCL1) and tumor necrosis factor α (TNF-α) concentrations after *ex vivo* LPS stimulation. Data were analysed using one-way ANOVA followed by Dunn's multiple comparisons test. * $p<0.05$, ** $p<0.01$, *** $p<0.001$.

Figure 1

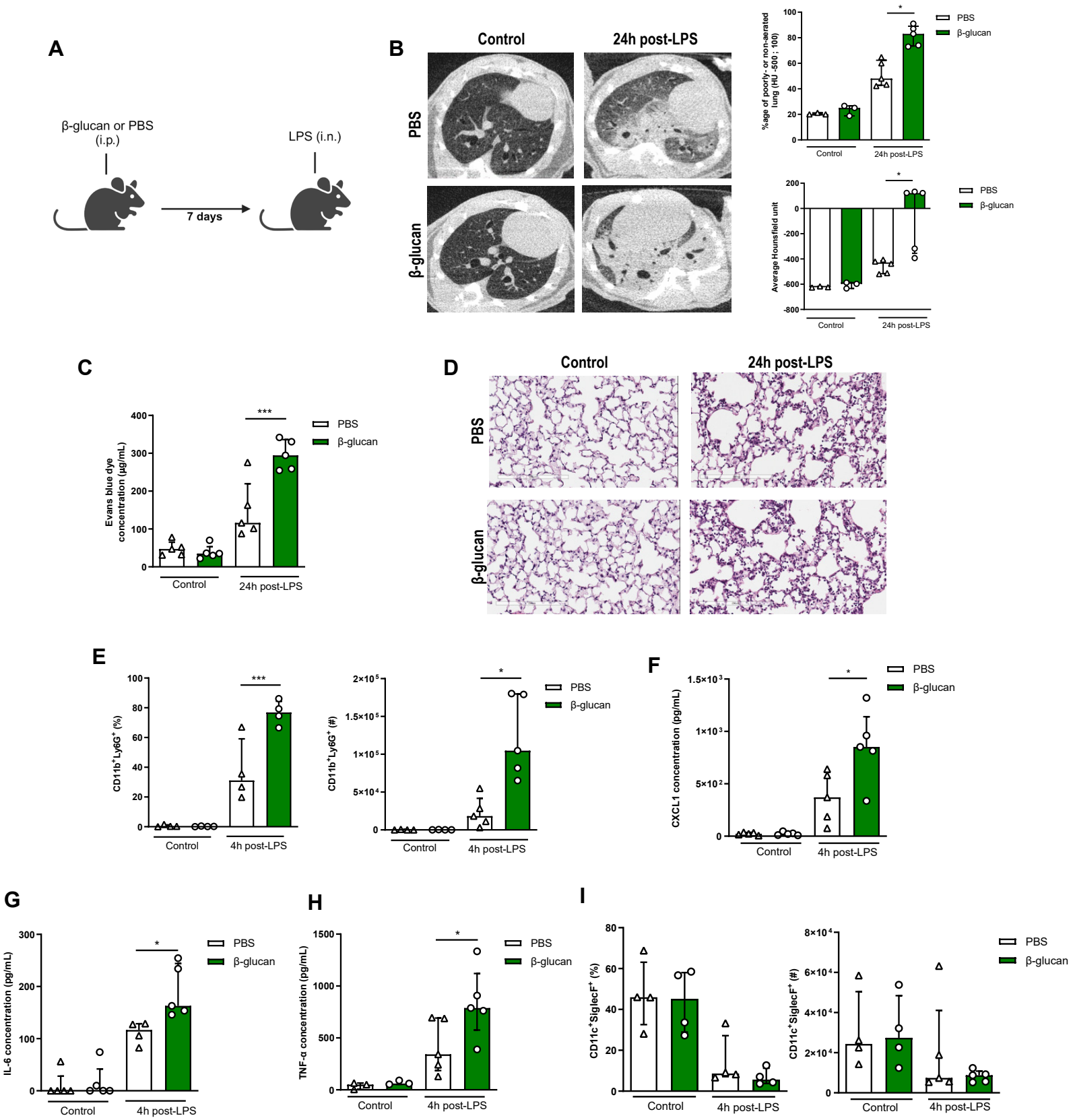
A
β-glucan or PBS (i.p.)
LPS (i.n.)
7 days
B
Control
24h post-LPS
PBS
β-glucan
%age of poorly- or non-aerated lung (HU -500 ; 100)
Average Hounsfield unit
C
Evans blue dye concentration (µg/mL)
D
E
CD11b+Ly6G+ (%)
CD11b+Ly6G+ (#)
4h post-LPS
F
CXCL1 concentration (pg/mL)
G
IL-6 concentration (pg/mL)
H
TNF-α concentration (pg/mL)
I
CD11c+SiglecF+ (%)
CD11c+SiglecF+ (#)

Figure 2

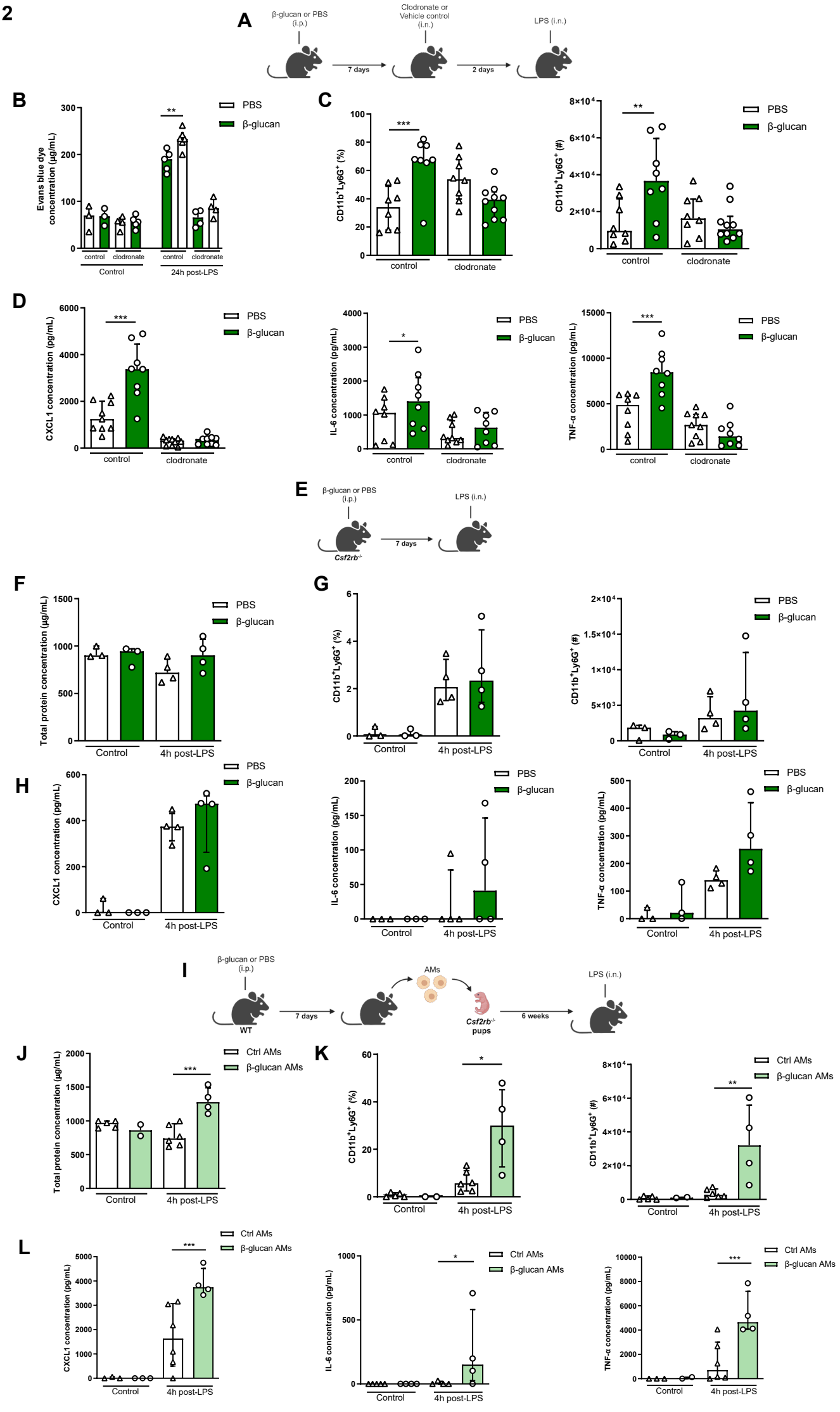
A
β-glucan or PBS (i.p.)
7 days
Clodronate or Vehicle control (i.n.)
2 days
LPS (i.n.)
B
Evans blue dye concentration (µg/mL)
PBS
β-glucan
control
clodronate
Control
24h post-LPS
C
CD11b+Ly6G+ (%)
CD11b+Ly6G+ (#)
D
CXCL1 concentration (pg/mL)
IL-6 concentration (pg/mL)
TNF-α concentration (pg/mL)
E
Csf2rb-/-
F
Total protein concentration (µg/mL)
G
H
I
WT
AMs
Csf2rb-/- pups
6 weeks
J
Ctrl AMs
β-glucan AMs
K
L

Figure 3

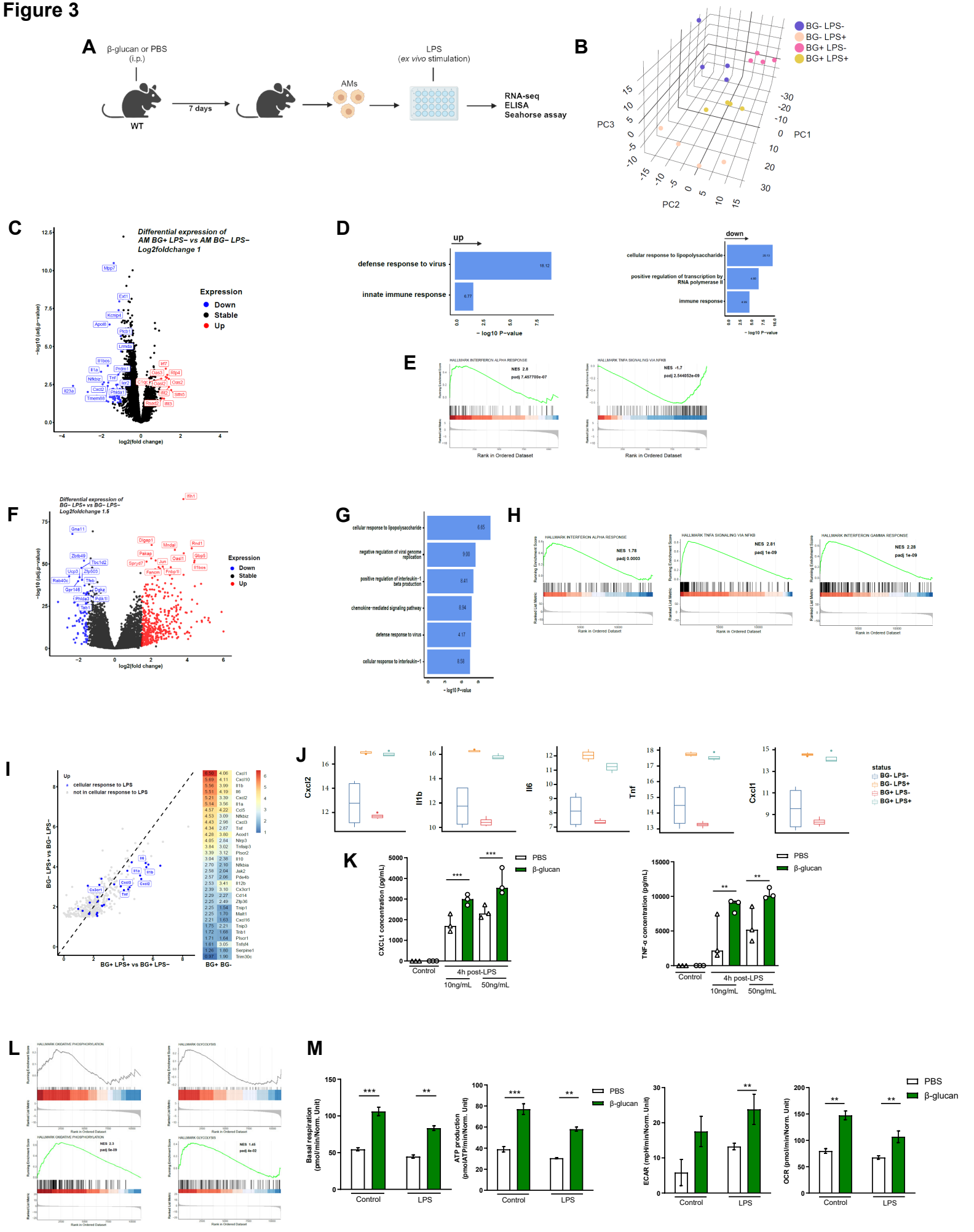
A
β-glucan or PBS
(i.p.)
WT
7 days
AMs
LPS
(ex vivo stimulation)
RNA-seq
ELISA
Seahorse assay
B
BG- LPS-
BG- LPS+
BG+ LPS-
BG+ LPS+
PC1
PC2
PC3
C
Differential expression of
AM BG+ LPS− vs AM BG− LPS−
Log2foldchange 1
Expression
Down
Stable
Up
−log10 (adj.p-value)
log2(fold change)
D
up
defense response to virus
innate immune response
− log10 P−value
down
cellular response to lipopolysaccharide
positive regulation of transcription by RNA polymerase II
immune response
E
HALLMARK INTERFERON ALPHA RESPONSE
NES 2.8
padj 7.457700e-07
HALLMARK TNFA SIGNALING VIA NFKB
NES -1.7
padj 2.544052e-09
Rank in Ordered Dataset
F
Differential expression of
BG− LPS+ vs BG− LPS−
Log2foldchange 1.5
Expression
Down
Stable
Up
−log10 (adj.p-value)
log2(fold change)
G
cellular response to lipopolysaccharide
negative regulation of viral genome replication
positive regulation of interleukin-1 beta production
chemokine-mediated signaling pathway
defense response to virus
cellular response to interleukin-1
− log10 P−value
H
HALLMARK INTERFERON ALPHA RESPONSE
NES 1.78
padj 0.0003
HALLMARK TNFA SIGNALING VIA NFKB
NES 2.81
padj 1e-09
HALLMARK INTERFERON GAMMA RESPONSE
NES 2.28
padj 1e-09
Rank in Ordered Dataset
I
Up
cellular response to LPS
not in cellular response to LPS
BG− LPS+ vs BG− LPS−
BG+ LPS+ vs BG+ LPS−
BG+ BG-
J
Cxcl2
Il1b
Il6
Tnf
Cxcl1
status
BG- LPS-
BG- LPS+
BG+ LPS-
BG+ LPS+
K
CXCL1 concentration (pg/mL)
PBS
β-glucan
Control
4h post-LPS
10ng/mL
50ng/mL
TNF-α concentration (pg/mL)
L
HALLMARK OXIDATIVE PHOSPHORYLATION
HALLMARK GLYCOLYSIS
NES 2.3
padj 5e-09
NES 1.45
padj 4e-02
M
Basal respiration (pmol/min/Norm. Unit)
ATP production (pmolATP/min/Norm. Unit)
ECAR (mpH/min/Norm. Unit)
OCR (pmol/min/Norm. Unit)
PBS
β-glucan
Control
LPS

Figure 4

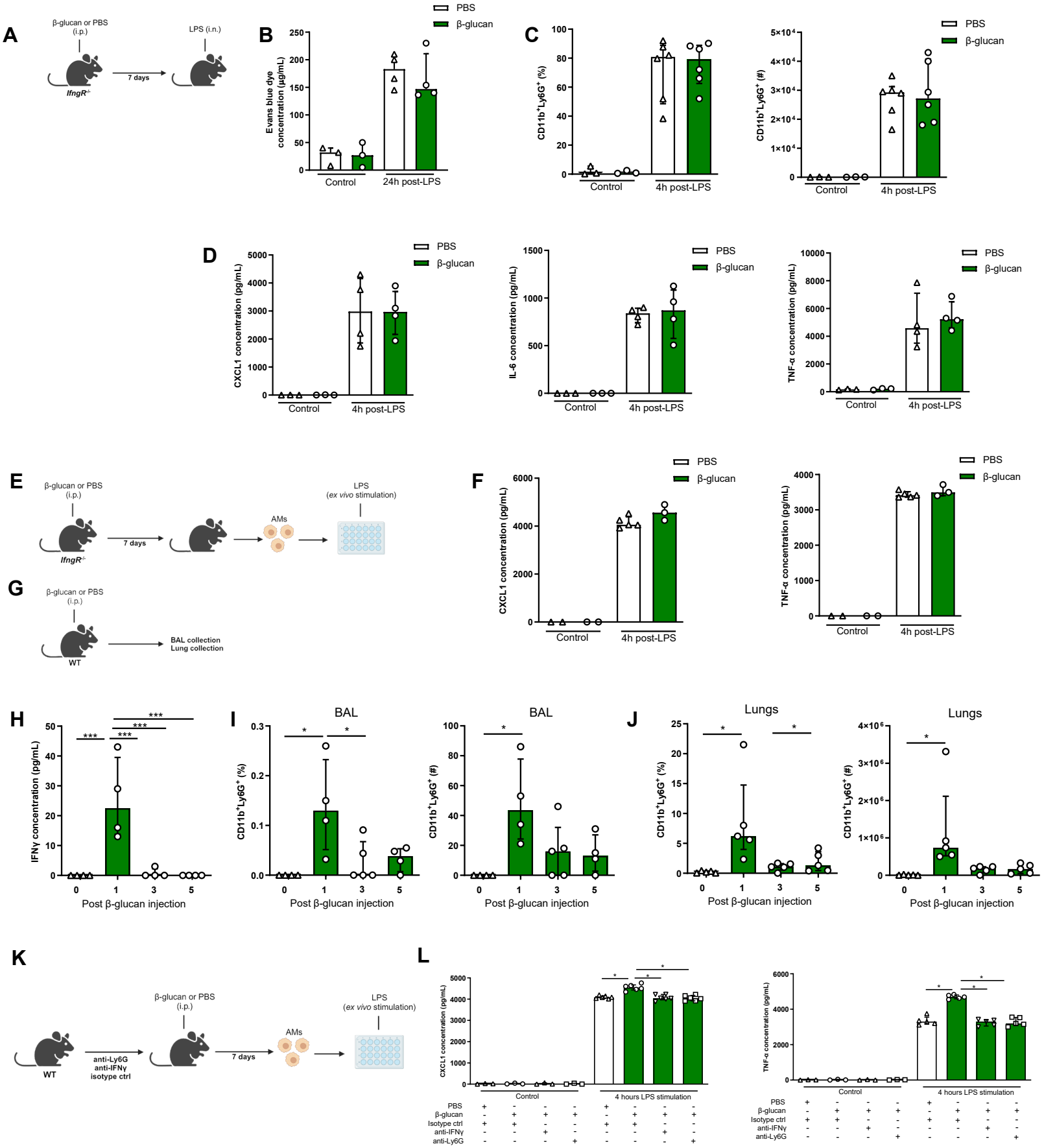
A
β-glucan or PBS (i.p.)
LPS (i.n.)
7 days
IfngR-/-
B
PBS
β-glucan
Evans blue dye concentration (µg/mL)
Control
24h post-LPS
C
CD11b+Ly6G+ (%)
CD11b+Ly6G+ (#)
Control
4h post-LPS
D
CXCL1 concentration (pg/mL)
IL-6 concentration (pg/mL)
TNF-α concentration (pg/mL)
E
LPS (ex vivo stimulation)
AMs
F
G
BAL collection
Lung collection
WT
H
IFNγ concentration (pg/mL)
Post β-glucan injection
I
BAL
J
Lungs
K
anti-Ly6G
anti-IFNγ
isotype ctrl
L
4 hours LPS stimulation
Isotype ctrl
anti-IFNγ
anti-Ly6G

Supplementary Figure 1

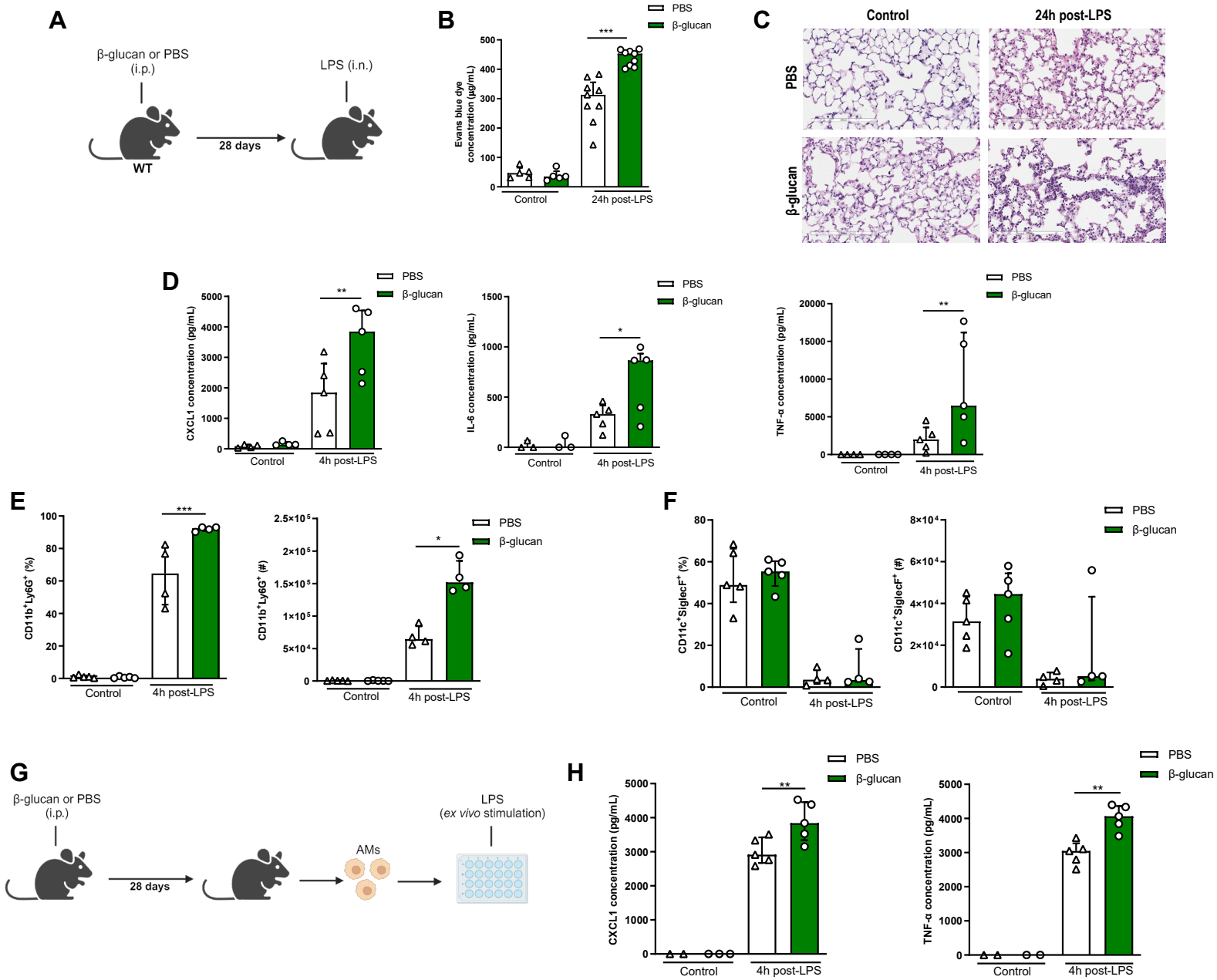

Supplementary Figure 2

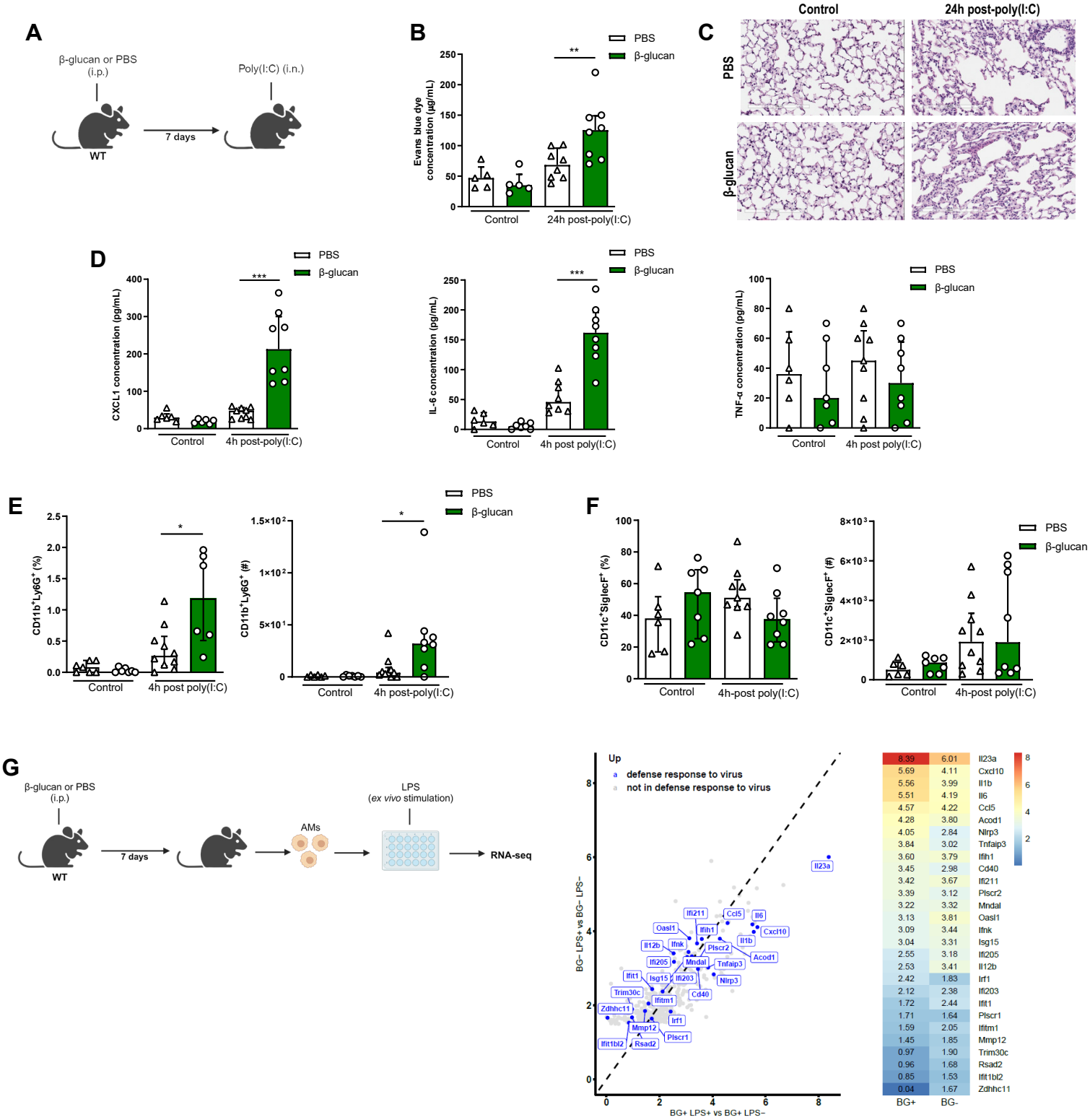
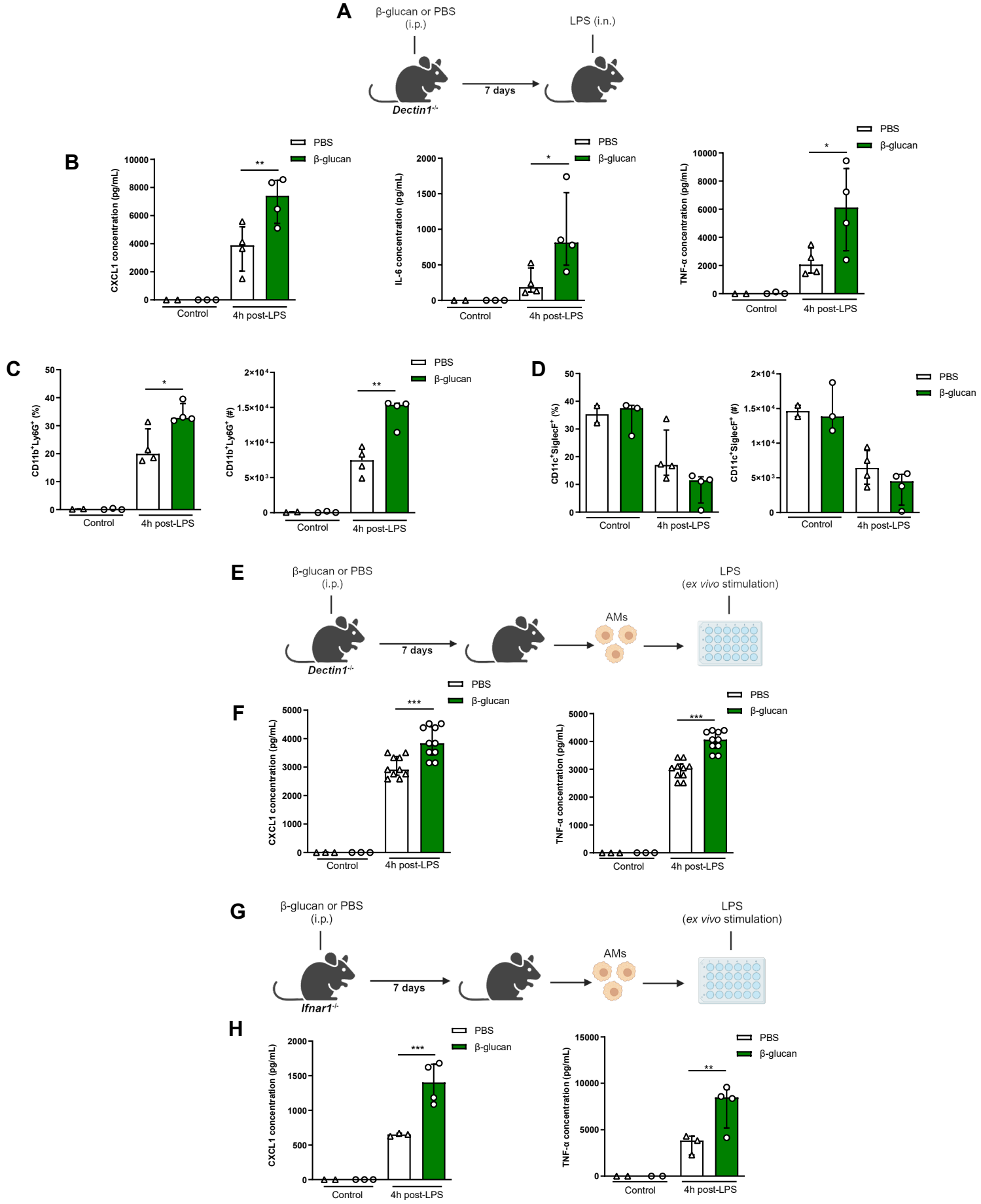
Supplementary Figure 3